New Journal of Physics

The open access journal at the forefront of physics

CrossMark

PAPER

Optically induced dynamic nuclear spin polarisation in diamond

Jochen Scheuer[1,2], Ilai Schwartz[2,3], Qiong Chen[2,3], David Schulze-Sünninghausen[4], Patrick Carl[5], Peter Höfer[5], Alexander Retzker[6], Hitoshi Sumiya[7], Junichi Isoya[8], Burkhard Luy[4], Martin B Plenio[2,3], Boris Naydenov[1,2] and Fedor Jelezko[1,2]

1   Institute of Quantum Optics, Ulm University, Albert Einstein Allee 11, D-89081 Ulm, Germany
2   Centre for Integrated Quantum Science and Technology (IQST), Albert Einstein Allee 11, D-89081 Ulm, Germany
3   Institute of Theoretical Physics, Ulm University, Albert Einstein Allee 11, D-89069 Ulm, Germany
4   Institute of Organic Chemistry and Institute for Biological Interfaces 4-Magnetic Resonance, Karlsruhe Institute of Technology (KIT), Fritz-Haber-Weg 6, D-76131 Karlsruhe, Germany
5   Bruker BioSpin GmbH, D-76287 Silberstreifen, Rheinstetten, Germany
6   Racah Institute of Physics, The Hebrew University of Jerusalem, Jerusalem 91904, Givat Ram, Israel
7   Sumitomo Electric Industries Ltd, Itami, 664-001, Japan
8   Research Centre for Knowledge Communities, University of Tsukuba,Tsukuba, 305-8550, Japan

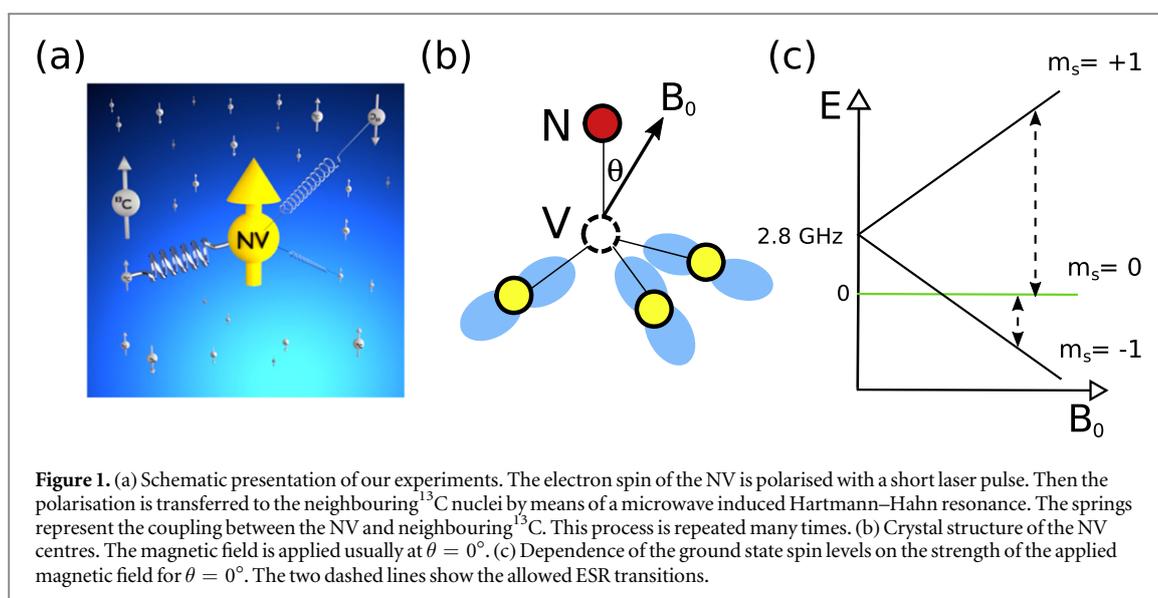E-mail: boris.naydenov@uni-ulm.de

Abstract

The sensitivity of magnetic resonance imaging (MRI) depends strongly on nuclear spin polarisation and, motivated by this observation, dynamical nuclear spin polarisation has recently been applied to enhance MRI protocols (Kurhanewicz *et al* 2011 *Neoplasia* **13** 81). Nuclear spins associated with the ^{13}C carbon isotope (nuclear spin $I = 1/2$) in diamond possess uniquely long spin lattice relaxation times (Reynhardt and High 2011 *Prog. Nucl. Magn. Reson. Spectrosc.* **38** 37). If they are present in diamond nanocrystals, especially when strongly polarised, they form a promising contrast agent for MRI. Current schemes for achieving nuclear polarisation, however, require cryogenic temperatures. Here we demonstrate an efficient scheme that realises optically induced ^{13}C nuclear spin hyperpolarisation in diamond at room temperature and low ambient magnetic field. Optical pumping of a nitrogen-vacancy centre creates a continuously renewable electron spin polarisation which can be transferred to surrounding ^{13}C nuclear spins. Importantly for future applications we also realise polarisation protocols that are robust against an unknown misalignment between magnetic field and crystal axis.

1. Introduction

Nuclear magnetic resonance (NMR) is one of the most powerful spectroscopic techniques with numerous applications in the life sciences, the material sciences and medicine. Long coherence times of nuclear spins allow to use this method for structural analysis of biomolecules and determination of molecular dynamics. Using highly sensitive NMR spectra combined with external magnetic field gradients nuclear magnetic moments can be imaged with high spatial resolution [1]. Both NMR spectroscopy and magnetic resonance imaging (MRI) critically depend on the polarisation of nuclear spins with which the observed signal scales linearly. At ambient conditions nuclear spins are very weakly polarised even in very high magnetic fields. Therefore significant effort was directed towards the development of protocols for enhancing nuclear spin polarisation above the thermal value.

Dynamic nuclear polarisation (DNP) protocols that use polarisation transfer from electron spins to nuclear spins have been realised and their application in imaging has been demonstrated recently [2]. It is important to note however that polarisation transfer reaches its best performance at low temperatures where electron spins are strongly polarised already in thermal equilibrium. Furthermore, owing to the long relaxation times of electron spins at these temperatures, typically a single polarisation cycle takes about a second during which a

Figure 1. (a) Schematic presentation of our experiments. The electron spin of the NV is polarised with a short laser pulse. Then the polarisation is transferred to the neighbouring ^{13}C nuclei by means of a microwave induced Hartmann–Hahn resonance. The springs represent the coupling between the NV and neighbouring ^{13}C. This process is repeated many times. (b) Crystal structure of the NV centres. The magnetic field is applied usually at $\theta = 0°$. (c) Dependence of the ground state spin levels on the strength of the applied magnetic field for $\theta = 0°$. The two dashed lines show the allowed ESR transitions.

single electron spin can polarise at most a single nuclear spin. Therefore a high concentration of polarising paramagnetic agent is required to reach a high degree of nuclear spin polarisation. These limitations create a significant demand on novel polarisation protocols that allow for fast and efficient polarisation transfer ideally even at room temperature. Recently a novel mechanism for DNP based on optically pumped electron spins (optical dynamical nuclear spin polarisation (ODNP) [3, 4]) was introduced and realised in molecular crystals. However the short lifetime of the photo-excited triplet state and fast dephasing of optically active impurities at ambient conditions limit the applicability of this technique for NMR and MRI. This is the reason why the recent demonstration of diamond [5–7] as a promising ODNP platform attracted the attention of the NMR and MRI communities.

The nitrogen-vacancy (NV) centre (see figure 1(b)) in diamond exhibits a long relaxation time of its electron spins even at room temperature [8] and its electronic ground state triplet can be efficiently polarised using optical excitation [5–7]. NVs can be created in bulk diamond using electron irradiation of nitrogen rich crystals or by controlled doping of ultra-pure diamonds using nitrogen ion implantation. Their wavefunction is localised to within 1 nm of these colour centres allowing them to retain these desirable physical properties when embedded in diamond nanocrystals with sizes below 10 nm [9]. Diamond nanoparticles doped with colour centres already found their application in fluorescence microscopy as non-bleachable fluorescence markers and drug carriers [10]. Recently nanodiamonds have been considered as promising material for applications related to DNP [5–7, 11–14]. See [15] for a recent review on biomedical applications of NV centres in nanodiamonds.

The reason why diamond is attractive for DNP and MRI applications is related to the long relaxation time of ^{13}C nuclear spins and ability to polarise them quickly using optically pumped colour centres. NVs can be polarised within 200 ns by a laser pulse that induces spin-selective relaxation into the $m_s = 0$ sublevel of the ground state resulting in spin polarisation exceeding 92% [16].

In order to transfer polarisation to nuclear spins it is necessary to match the energy scale of the electron spin to that of the nuclear spin systems because the large energy mismatch between these two spins species due to the zero-field splitting ($D = 2.8$ GHz) of the spin triplet of NV centre prevents a direct polarisation exchange between the electron and nuclear spins. There are several methods to bring electron and nuclear spins in resonance. The first one is to set the static magnetic field close to the level crossing either the ground [17] or the excited state of the NV centre [18, 19]. Resonance can also be achieved by microwave driving of the electron spin of the NV with a Rabi frequency that matches the nuclear spin Larmor frequency (Hartmann–Hahn condition) [19, 20]. Furthermore it is possible to realise polarisation transfer by the solid effect (driving a forbidden double quantum transition thus inducing electron and nuclear spin flips) [5, 14]. Although the above mentioned techniques perform well for bulk diamond where NV centres have well defined orientations with respect to the static and driving fields, they do not apply directly to nanodiamond samples due to their random orientations. The strong spread of the Rabi frequencies of the microwave for chaotically oriented nanodiamonds severely reduces the probability to reach a Hartmann–Hahn resonance. Furthermore, the application of the solid effect would require an integration over a very wide range of detunings due to the large Zeeman shifts that are experienced by the NV centre. Both effects will result in a severe reduction of the total achievable nuclear spin polarisation. In this work we demonstrate the experimental realisation of a novel robust technique based on a fast sweep of the microwave driving field which induces a Landau–Zener transition [14] that has been designed
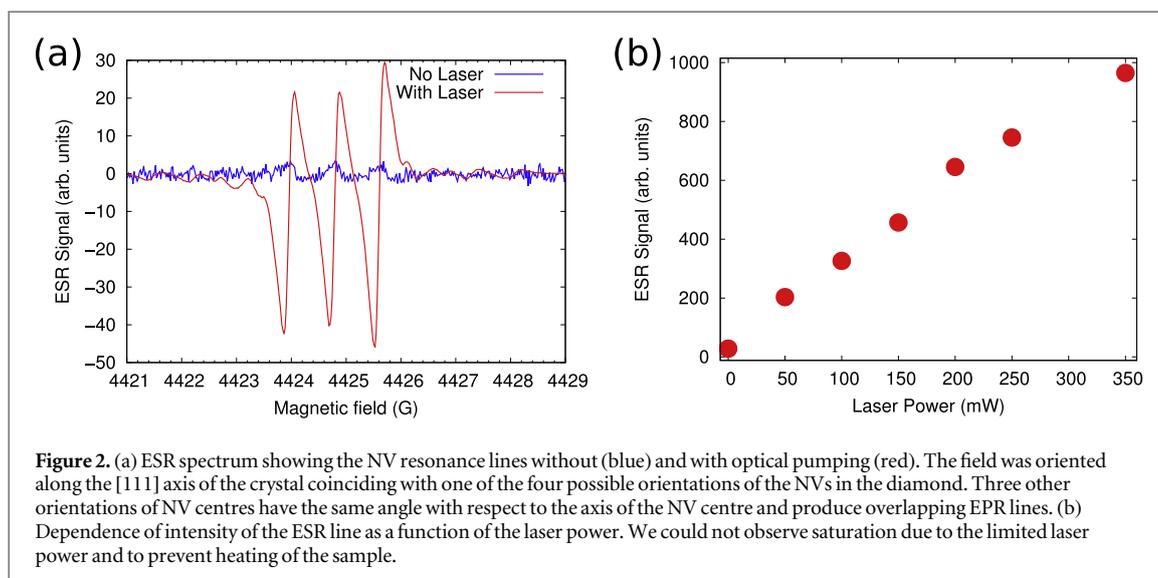
Figure 2. (a) ESR spectrum showing the NV resonance lines without (blue) and with optical pumping (red). The field was oriented along the [111] axis of the crystal coinciding with one of the four possible orientations of the NVs in the diamond. Three other orientations of NV centres have the same angle with respect to the axis of the NV centre and produce overlapping EPR lines. (b) Dependence of intensity of the ESR line as a function of the laser power. We could not observe saturation due to the limited laser power and to prevent heating of the sample.

specifically to achieve significant nuclear spin polarisation even in the presence of random orientations of nanodiamonds.
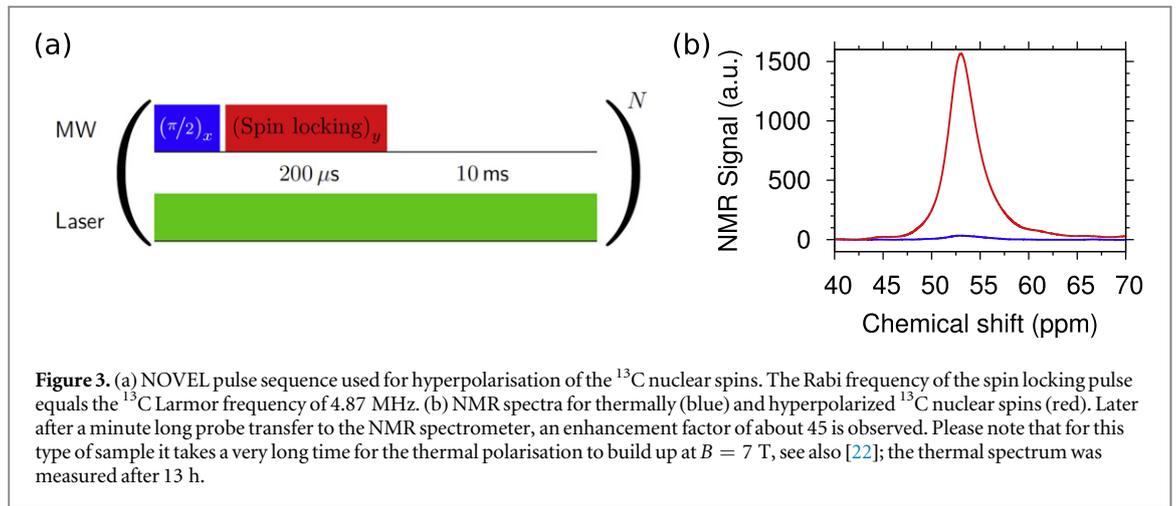
2. Experiments

The experiments reported in this paper were performed on a synthetic diamond with natural abundance of ^{13}C nuclear spins (1.1%). The crystal was grown using the high pressure high temperature technique and contains 0.5 ppm P1 centres (a paramagnetic defect which is constituted by a single substitutional nitrogen atom). About 10% of the P1 centres were converted to NV centres by high energy electron irradiation and subsequent annealing, achieving NV concentration of 0.05 ppm. Figure 1(a) shows a sketch of the DNP experiment.

The ODNP was performed on a commercial X band electron paramagnetic resonance (EPR) spectrometer (Bruker ELEXYS II) equipped with an arbitrary waveform generator and a microwave cavity allowing optical access. In order to polarise the NV centres a continuous laser beam (Laser quantum, Gem with a wavelength of 532 nm) with 3 mm diameter and 150 mW power was directed onto the crystal inside the EPR resonator. Owing to the weak NV-doping of the sample the optical density of the crystal was low (below 0.1). This allows homogeneous illumination of the sample resulting in similar polarisation conditions for the whole ensemble of NV centres. In figure 2(a) the enhancement of the EPR spectrum of NVs in diamond under continuous laser irradiation is shown.

As a first test of DNP we have performed polarisation transfer from NV centres to ^{13}C using the Hartmann Hahn resonance at room temperature. This protocol, called nuclear spin orientation via electron spin locking (NOVEL) [21], brings the electron spin of the NV centre in resonance with the surrounding nuclear spins when the driving frequency of the electron spin (Rabi frequency) equals the Larmor frequency of the nuclear spins. We have previously shown that the nuclear spin polarisation resulted in narrowing of the NV's ESR line width. Such a narrowing is related to polarisation of strongly coupled nuclear spins in its surrounding (so called 'frozen core') [19]. For experiments presented in this paper we were focusing on studies of the polarisation of bulk nuclear spins which is relevant for future applications of nanodiamonds as contrast agents in NMR and MRI. Therefore the polarisation was not measured using NV centre probes, but rather by using a conventional NMR spectrometer (Bruker Fourier 300). Figure 3(a) shows the experimental sequence for Hartmann–Hahn DNP.

It consists of an electron spin locking combined with continuous illumination of the NV centres. Note that the illumination with power density of 10 W cm^{-2} induces optical pumping at kHz rate. Therefore dephasing related to optical pumping is negligible within the duration of the spin locking pulse. The length of the latter is limited by the relaxation time of the NV electron spin in the rotating frame ($T_{1\rho} = 0.465$ ms, data not shown). In our experiments a value of 0.2 ms was used.

A single NV centre can polarise one nuclear spin within one polarisation transfer cycle. In our crystal the concentration of ^{13}C nuclear spins (1.1%) was exceeding by four orders of magnitude the concentration of NV defects. Therefore in order to achieve strong nuclear spin polarisation it was necessary to apply multiple repetitions of the Hartmann–Hahn protocol. Another important condition for efficient bulk polarisation is the ability to transfer polarisation to nuclei beyond the frozen core. This can be achieved by polarising nuclear spins at the edge of the frozen core sphere to allow for the diffusion of nuclear spin polarisation. Spin diffusion enabled

Figure 3. (a) NOVEL pulse sequence used for hyperpolarisation of the ^{13}C nuclear spins. The Rabi frequency of the spin locking pulse equals the ^{13}C Larmor frequency of 4.87 MHz. (b) NMR spectra for thermally (blue) and hyperpolarized ^{13}C nuclear spins (red). Later after a minute long probe transfer to the NMR spectrometer, an enhancement factor of about 45 is observed. Please note that for this type of sample it takes a very long time for the thermal polarisation to build up at $B = 7$ T, see also [22]; the thermal spectrum was measured after 13 h.

by dipole–dipole interaction between the nuclear spins will then lead to polarisation transfer to nuclei in the bulk. Note that the spin diffusion is slowed down by the magnetic field gradient created by the NV centres that are in the $m_s = +1$ and $m_s = -1$ state. To ameliorate conditions for diffusion we have introduced a polarisation transfer time window during which the NV centre is initialised into the $m_s = 0$ state, where there is no coupling to nuclei. During this time interval polarised nuclei in the frozen core can transfer their polarisation by diffusion to the volume outside the frozen core. The length of the spin locking pulse in the NOVEL sequence was chosen to reach nuclear spins with coupling constant of 10 kHz (situated approximately in a 2 nm radius around the NV centre). After 5 min of polarisation the sample was removed from the EPR spectrometer manually and transferred to the NMR spectrometer for measuring the ^{13}C NMR signal. During the transfer, that took about a minute time across a distance of approximately 100 m, the sample was kept in a static magnetic field (with a strength of few hundred Gauss) created by a permanent magnet. Figure 3(b) shows NMR spectra of non-polarised (blue line) and polarised (red line) nuclear spins. The former has been recorded after keeping the sample for 13 h in the spectrometer at a magnetic field of 7 T in order to let the thermal polarisation build-up. If the sample is measured directly after inserting it into the spectrometer no signal is observed in contrast to the polarised sample. Our hyperpolarisation procedure takes about 6 min, resulting in a factor of at least 130 reduction of the measurement time. Additionally we have observed a 45 fold enhancement of the signal which is in good agreement with expected polarisation enhancement (see the supplementary information for details about the simulation and measurement of the polarisation build-up). We estimate that this enhancement corresponds to a nuclear spin polarisation of 0.054%, when we assume that thermal polarisation is reached after keeping the sample 13 h in the NMR spectrometer.
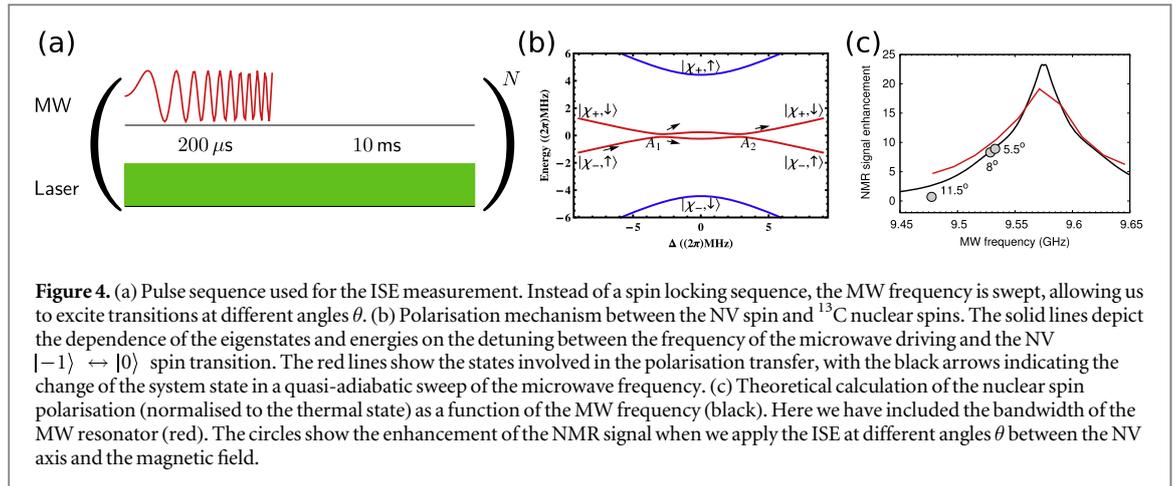
A technique allowing to polarise nuclear spins in diamond is of particular interest for applications in MRI of diamond nanocrystals as labels. However, as stated earlier, in samples with random orientations, e.g. in suspensions, the Hartmann–Hahn condition is achieved only for the tiny subensemble for which the quantisation axes of NV centres are aligned with the external magnetic field. Recently, a new approach has been proposed that optimises the integrated solid effect (ISE) for randomly oriented NV centres [14].

This method is based on a quasi-adiabatic sweep of the driving field frequency and allows efficient population transfer for a wide range of misalignment angles (angle θ between the axis of the NV centre, see figure 1(b), and the external magnetic field). The pulse sequence is shown in figure 4(a).

For illustrating the basic idea, let us consider a system that is composed of a NV centre and a single ^{13}C nuclear spin in a nanodiamond of random orientation, where θ is the misalignment angle between the NV-axis and the magnetic field. In a strong magnetic field along the z-direction ($\gamma_e B \gg D$, with $\gamma_e B$ denoting the electron Larmor frequency, and D the NV centre zero-field splitting), the quantisation axis is given by the magnetic field, with the zero field splitting acting as a perturbation (see [14] and supplementary information). Focusing on the $\{\,|-1\rangle,\,|0\rangle\,\}$ subspace of the NV centre, we now apply a microwave driving $\sqrt{2}\,\Omega S_x \cos \omega_M t$ corresponding to the NV centre spin transitions $|-1\rangle \leftrightarrow |0\rangle$, ($\sqrt{2}\,\Omega$ is the Rabi frequency of the driving field and ω_M its frequency. In the rotating frame with the driving field frequency ω_M, the Hamiltonian can be written as

$$H_{\text{trans}} = \Omega \sigma_z + \Delta \sigma_x + B_{\text{eff}} I_z + a_z \sigma_z I_z + a_x \sigma_x I_x,$$

where $\Delta = D(\theta) - \delta(\theta) - \gamma_e B + \omega_M$ is the detuning between the driving frequency and the NV $|-1\rangle \leftrightarrow |0\rangle$, spin transition ($D(\theta)$, $\delta(\theta)$ are the angle dependent effects of the zero-field splitting, see supplementary information). $B_{\text{eff}} = \gamma_n B - A$, with γ_e, γ_n being the electron and nuclear gyromagnetic ratios,

Figure 4. (a) Pulse sequence used for the ISE measurement. Instead of a spin locking sequence, the MW frequency is swept, allowing us to excite transitions at different angles θ. (b) Polarisation mechanism between the NV spin and ^{13}C nuclear spins. The solid lines depict the dependence of the eigenstates and energies on the detuning between the frequency of the microwave driving and the NV $|-1\rangle \leftrightarrow |0\rangle$ spin transition. The red lines show the states involved in the polarisation transfer, with the black arrows indicating the change of the system state in a quasi-adiabatic sweep of the microwave frequency. (c) Theoretical calculation of the nuclear spin polarisation (normalised to the thermal state) as a function of the MW frequency (black). Here we have included the bandwidth of the MW resonator (red). The circles show the enhancement of the NMR signal when we apply the ISE at different angles θ between the NV axis and the magnetic field.

and a_z, a_x are the elements of the secular and pseudo-secular hyperfine interactions respectively. $\vec{I}$ is the nuclear spin-1/2 operator and σ_z, σ_x are 1/2 times the Pauli matrices in the $|\pm\rangle = 1/\sqrt{2}\,(|0\rangle \pm |-1\rangle)$) basis.

Figure 4(b) shows the dependence of eigenstates of this Hamiltonian on the detuning, with $|\chi_\pm\rangle = \cos\zeta\,|-\rangle \pm \sin\zeta\,|+\rangle$ denoting the eigenstates, $\tan^{-1}(\zeta/2) = \Delta/\Omega$. We note two resonance points A_1 and A_2. The polarisation is transferred between the dressed state of the electron spin and the nuclear spin during a quasi-adiabatic sweep through these resonances (see supplementary information for additional details). Note that the sweep rate should be non-adiabatic compared to the dipolar coupling (typically 50–200 kHz) time constant between electron and nuclear spins, i.e. around the resonance points A_1 and A_2. The upper limit on the sweep parameter is defined by the Rabi frequency of the microwave field determining the splitting between the red and blue lines in figure 4(b). Exceeding the latter would lead to the randomisation of nuclear spin polarisation.

Owing to long sample transfer time, and the limited ^{13}C relaxation time in nanodiamonds of a few minutes [23] (we observed similar values, data not shown) compared to hours for the latter at $B = 7$ T, our demonstrations were performed on bulk diamonds rather than in nano-diamonds. In order to realise a misalignment between NV-axis and external magnetic field, experiments were performed using different orientations of the diamond crystal with respect to the external static field but without change of the polarisation protocol. In our experimental conditions the sweep rate was chosen to be 0.3 MHz μs^{-1} and the sweep range was 100 MHz This allows to cover a misalignment angle of about $10°$ corresponding to a $\sim$2% fraction of colour centres for isotropic orientation of NV axes, and would result in a fast build-up of polarisation in nanodiamonds, as shown by detailed numerical simulations [14]. According to the latter it is possible to reach 20% polarisation for a nanodiamond with a spherical shape and a radius of 5 nm.

The experiment has been performed as in the case of NOVEL. We polarise the samples for 5 min. and then transfer the diamond to the NMR spectrometer where we measure the ^{13}C signal. The observed polarisation enhancement is demonstrated in figure 4(c). Note that slightly lower efficiency of polarisation transfer at strong misalignment angles is related to non-optimal drive at high detuning. In our experiments the microwave drive generated by an arbitrary waveform generator was kept at constant amplitude, but the microwave resonator bandwidth was limited to about 100 MHz half width at half maximum. Therefore at high rotation angle (corresponding to the resonance at the edge resonator band), the effective coupling by matching the resonance condition is much lower.

The theoretical expected polarisation enhancement was computed based on the calculated polarisation transfer probability of the ISE:

$$\bar{P} = 2P_{LZ}\left(1 - P_{LZ}\right),$$

$$P_{LZ} = e^{-2\pi\mu}, \quad \mu = \frac{\Omega^2 a_{x'}^2}{16\nu\left(\gamma_n B\right)\sqrt{\left(\gamma_n B\right)^2 - \Omega^2}}.$$

With Ω denoting the Rabi frequency, $a_{x'}$ the effective dipolar coupling, ν the frequency sweep rate, and $\gamma_n B$ the nuclear Larmor frequency. The polarisation rate, which depends on the cycling time, is then averaged over an ensemble for a nuclear spin bath of 500 spins around the NV centre, and a steady-state polarisation depending on the ^{13}C relaxation time in the EPR magnetic field (see supplementary material stacks.iop.org/NJP/18/013040/mmedia). Nuclear spin diffusion is limited by the dipolar coupling between the ^{13}C spins (2 kHz for

next neighbours) and it does not seem to be a bottleneck of the polarisation build-up in our experiments, due to the 10 ms polarisation transfer time between cycles with the NV in the $m_s = 0$ state.

3. Conclusions

Our results show that optical nuclear spin polarisation in diamond can be performed for a wide range of orientations of NV centres at room temperature. Our protocol based on quasi-adiabatic sweep of microwave field across the resonance points makes it possible to polarise diamond nanoparticles. Such functionalised diamond nanocrystals can serve as agent for molecular imaging using MRI techniques. Our method can be in principle transferred to other nanoparticles containing electron spins that can be optically polarised.

Acknowledgments

References

[1] Lauterbur P C 1973 Image formation by induced local interactions—examples employing nuclear magnetic-resonance *Nature* **242** 190–1
[2] von Morze C *et al* 2014 Simultaneous multiagent hyperpolarized C-13 perfusion imaging *Magn. Reson. Med.* **72** 1599–609
[3] Sukhenko S A and Salikhov K M 1985 Calculations of optical nuclear-spin polarizations for randomly oriented molecules *Chem. Phys.* **98** 431–6
[4] Tateishi K *et al* 2014 Room temperature hyperpolarization of nuclear spins in bulk *Proc. Natl Acad. Sci. USA* **111** 7527–30
[5] London P *et al* 2013 Detecting and polarizing nuclear spins with double resonance on a single electron spin *Phys. Rev. Lett.* **111** 067601
[6] Álvarez G A *et al* 2015 Local and bulk 13C hyperpolarization in nitrogen-vacancy-centred diamonds at variable fields and orientations *Nat. Commun.* **6** 8456
[7] King J P *et al* 2015 Room-temperature *in situ* nuclear spin hyperpolarization from optically-pumped nitrogen vacancy centers in diamond *Nat. Commun.* **6** 8965
[8] Doherty M W *et al* 2013 The nitrogen-vacancy colour centre in diamond *Phys. Rep.* **528** 1–45
[9] Tisler J *et al* 2009 Fluorescence and spin properties of defects in single digit nanodiamonds *ACS Nano* **3** 1959–65
[10] Mochalin V N *et al* 2012 The properties and applications of nanodiamonds *Nat. Nanotechnology* **7** 11–23
[11] Casabianca L B *et al* 2011 Factors affecting DNP NMR in polycrystalline diamond samples *J. Phys. Chem. C* **115** 19041–8
[12] Ewa Rej T G, Boele T, Waddington D E J and Reilly D J 2015 Hyperpolarized nanodiamond with long spin relaxation times *Nat. Commun.* **6** 8459
[13] King J P, Coles P J and Reimer J A 2010 Optical polarization of C-13 nuclei in diamond through nitrogen vacancy centers *Phys. Rev. B* **81** 073201
[14] Chen Q *et al* 2015 Optical hyperpolarization of 13C nuclear spins in nanodiamond ensembles arXiv:1504.02368
[15] Wu Y *et al* 2015 Diamond quantum devices in biology *Angew. Chem. Int. Ed. Engl.* in press
[16] Waldherr G *et al* 2011 Dark states of single nitrogen-vacancy centers in diamond unraveled by single shot NMR *Phys. Rev. Lett.* **106** 157601
[17] Wang H J *et al* 2013 Sensitive magnetic control of ensemble nuclear spin hyperpolarization in diamond *Nat. Commun.* **4** 1940
[18] Jacques V *et al* 2009 Dynamic polarization of single nuclear spins by optical pumping of nitrogen-vacancy color centers in diamond at room temperature *Phys. Rev. Lett.* **102** 057403
[19] Fischer R *et al* 2013 Bulk nuclear polarization enhanced at room temperature by optical pumping *Phys. Rev. Lett.* **111** 057601
[20] Cai J-M *et al* 2013 Diamond based single molecule magnetic resonance spectroscopy *New J. Phys.* **15** 013020
[21] Henstra A *et al* 1988 Nuclear spin orientation via electron spin locking (NOVEL) *J. Magn. Reson.* **77** 389
[22] Reynhardt E C and High G L 2011 *Prog. Nucl. Magn. Reson. Spectrosc.* **38** 37
[23] Panich A M *et al* 2015 Size dependence of 13C nuclear spin-lattice relaxation in micro- and nanodiamonds *J. Phys.: Condens. Matter* **27** 072203